Scientific Research Publishing

American Journal of Computational Mathematics, 2024, 14, 189-202
https://www.scirp.org/journal/ajcm
ISSN Online: 2161-1211
ISSN Print: 2161-1203

# Simulation of Air Flow along Human Lung for Cylindrical Channel of Porous Medium

**Sadiya Akhter[1], Mahtab Uddin Ahmmed[2]**

[1]Department of Quantitative Sciences, International University of Business Agriculture and Technology, Dhaka, Bangladesh
[2]Department of Mathematics, Jahangirnagar University, Dhaka, Bangladesh
Email: sadiyarahmansm@gmail.com, mahtab.ahmmed@gmail.com

**How to cite this paper:** Akhter, S. and Ahmmed, M.U. (2024) Simulation of Air Flow along Human Lung for Cylindrical Channel of Porous Medium. *American Journal of Computational Mathematics*, **14**, 189-202.
https://doi.org/10.4236/ajcm.2024.142006

**Received:** March 26, 2024
**Accepted:** May 14, 2024
**Published:** May 17, 2024



## Abstract

The steady flow behavior in terminal bronchus of human lung for cylindrical channel of porous medium has been studied. The governing equations have been solved analytically and numerically for cylindrical channel. Finite difference method is incorporated to simulate the problem. The numerical results are compared with square duct channel for different parametric effect. It is observed that the flow rate is increased in cylindrical channel compared to square duct channel for the increasing value of pressure gradient, porosity and permeability. On the contrary, the flow rate is decreased in square duct channel compared to cylindrical channel for increasing value of viscosity. Flow rate in both channels is analyzed and compared for non-porous medium also. It is observed that flow rate is increased very high in cylindrical channel compared to square duct channel for both medium.

## Keywords

Human Lung, Cylindrical Channel, Square Duct Channel, Terminal Bronchus, Porosity

## 1. Introduction

Gas exchange procedure in human respiratory system plays a vital role in biomedical science. Most of the investigations in this field are related with drug delivery, diagnostics of pulmonary disease and chronic bronchitis. In natural process the respiratory system is fully inferred but according to dynamic behavior of fluid the explanation of gas exchange process in human lung is very challenging because of complex asymmetric and irregular shape of lung. A computational study is approached to know the unsteady flow behavior in the respiratory channel of human lung [1]. Here the numerical results were calculated for normal breath-

ing condition and maximal exercise condition and it was found that the both conditions were fully depended on convective effect and viscosity effect. In human upper airways, the inspiration and expiration from trachea to the sixth generation are simulated numerically [2]. Here at the time of expiration air enters into the right center of trachea from the upper lobar bronchus and struck airflow from lower and center right bronchi, so that the streamlines of trachea positions at inspiration and expiration are switched. The flow characteristics have been numerically investigated in three generation bifurcation airways by using control volume method [3]. In that paper, they established the relation between flow characteristics and Reynolds number including pressure drop and flow patterns. The air flow in human lung with high frequency oscillatory ventilation (HFOV) was performed experimentally and numerically [4]. In that work, the flow convection in lower airways were investigated and obtained physical perception of old air deportation. Flow behavior in $11^{th}$ generation of human lung through square duct of porous medium has been investigated [5]. On that work flow rate was shown for different parametric effect as pressure gradient, porosity, permeability and viscosity. The characteristics of air flow in bifurcating airway and mass transfer through porous media of human lung has been investigated [6]. Here the resistance of mass transfer between blood and trachea in the capillaries was acquired depending on porous media approach. Coupled fluid porous system is an important method to examine flow simulation in human lung channel [7]. In that paper, simulation of pore level is showed in alveolate duct geometry to determine its permeability. Air flow in an alveolate duct has been shown by a theoretically based closure model [8]. Here the permeability is obtained by solving the closure problem and direct simulation of flow obtained by verifying the assumptions. The blood flow and water movement in the channel of porous wall were discussed [9]. In that work numerical results were presented in terms of velocity and pressure distribution. The air flow in a cylinder with permeable wall is investigated experimentally [10]. Here it is observed that the air flow through nozzle is axisymmetric and the hotter layers are distinguished from permeable cold layers. The air flow in human tracheal cartilaginous rings of cylindrical hills has been studied [11]. In that paper Large Eddy Simulation (LES) is used to know airflow in cartilaginous rings at Reynolds number of 5176 in trachea region. The removal of particles from cylindrical and rectangular channel using image force has been studied [12]. Here it is found that the results in cylindrical channel are appropriate with particle deposition in human lung airways. In cylindrical coordinate system the highly energy conservative second order finite difference method is used [13]. Here the numerical results have shown in different schemes for inviscid flow for both equally spaced and unequally spaced meshes. The three-dimensional incompressible flow is shown in cylindrical channel using finite difference scheme [14]. Here the flow is simulated for cylindrical channel with time dependent three-dimensional Navier-Stokes equation using finite difference method.

In this paper the flow behavior is shown in 11th generation of human lung for cylindrical channel of porous medium. The flow rate is measured with different parametric effect as pressure gradient, porosity, permeability and viscosity. The numerical results are compared with square duct channel for porous and non-porous medium. It is observed that for both medium the flow rate is much more in cylindrical channel compared to square duct channel.

## 2. Anatomy and Function of Lung

The lungs are important organs in the respiratory system that participate in gas exchange process. Air is inhaled through nose or mouth and then instantly passes to pharynx. During gas exchange task, the lung influences a very large inner surface to conduct airflows in the gas exchange area. In gas exchange process, oxygen is carried from lungs to the bloodstream. Human lung has a branching tree structure consists of trachea, bronchi and bronchioles (Figure 1).

Throughout the lung development, the conducting airways are structured by the generation and growth of the gas exchange area. In right and left lungs, the number of alveoli is compared with age, height and weight. During first 2 years of life the number of alveoli in human lung is increased exponentially. From childhood (age of 6 years) to adulthood the small bronchioles and alveoli expand in size to increase the lung volume. The total number of alveoli in human adult lung is about 480 million and number of alveoli is closely connected to the total lung volume, large lungs having noticeably more alveoli. Lung is generally known for its gas exchange function; it is exhibited to signals in inhaled air and

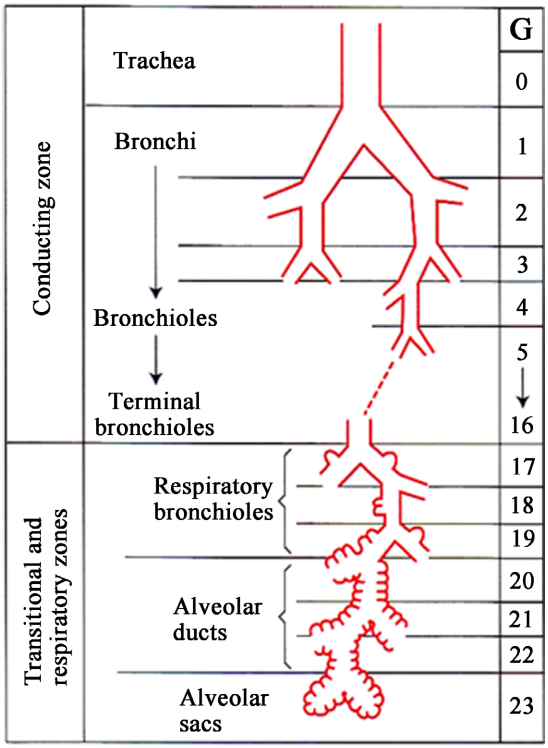


Figure 1. Airway branching of human lung (Weibel, 1963).

reacts to them by cooperating with other systems together with immune cells and the neural circuit. The air, blood and tissue these three components formulate the gas exchange region. The tissue compartments consequence as a structure of two dimension and constantly affecting components, air and blood.

The branching tree structure has approximately 23 branches or generations from the trachea (generation 0) to the last order of terminal bronchioles (generation 23). An adult trachea has a length of 12 cm and diameter 1.8 cm. The right bronchus is being wider and makes smaller angle with axis of trachea which bifurcates asymmetrically. The diameter of small bronchi (G5 to G11) is continuously falling from 3.5 mm to 1 mm. In $11^{th}$ generation there is an important change occurs where the length is about 3.90 mm and diameter is about 1.09 mm. It is a conducting zone where the number of branches is 2048 and Re number is approximately 10 - 12 as shown in Table 1. In tracheobronchial tree the average diameter decreases in each generation. The diameter of each alveolus is 0.2 - 0.3 mm. The respiratory zone consists of bronchioles, alveolar ducts and alveolar sacs (G17 to G23) where diffusion and conduction take place in gas transportation. The respiratory system consists of upper airways and lower airways. The upper airways include pharynx, nasal passages and paranasal sinuses. In gas exchange process the respiratory tract can be divided into conducting zone and respiratory zone. The lower respiratory tract contains trachea, mainstream bronchus, lobar bronchus, segmental bronchus, bronchiole, alveolar duct and alveolus. The lower respiratory tract is actually the tracheobronchial tree which supplies air to the lungs. In lung structure model the respiratory bronchioles contain 2.5 to 3 liters of air where an adult lung can contain almost 5 liters of air.

## 3. Equation and Formulation of the Problem

### 3.1. Porous Medium

We consider the cylindrical channel for steady flow behavior in $11^{th}$ generation of human lung as shown in Figure 2. Hydraulic diameters are maintained in cylindrical channel and square duct channel in our simulation. The walls of the cylinder are porous with uniform permeability.

We introduce Darcy resistance $R$ as

$$R = \frac{-\mu\varphi}{k} v \tag{1}$$

where $v$ is flow rate, $\mu$ is viscosity, $\varphi$ is the porosity of the fluid and $k$ is permeability.

We consider the cylindrical co-ordinate $(r,\theta,z)$ with $z$ axis co-incident with the common axis of the cylinder. For steady flow the equations governing the flow are the continuity and momentum equations as

$$\frac{1}{r}\frac{\partial}{\partial r}(rv_r)+\frac{1}{r}\frac{\partial v_\theta}{\partial \theta}+\frac{\partial v_z}{\partial z}=0 \tag{2}$$

$r$-momentum

**Table 1.** Approximate quantification of the human bronchial system (Weibel's model).

| | Generation (G) | Number (n) | Length (mm) | Mean diameter (mm) | Re |
|---|---|---|---|---|---|
| Trachea | 0 | 1 | 120.00 | 18.00 | 1480 |
| Main Bronchus | 1 | 2 | 47.60 | 12.20 | 1092 |
| Lobar Bronchus | 2 | 4 | 19.00 | 8.30 | 803 |
| | 3 | 8 | 7.60 | 5.60 | 595 |
| Segmental Bronchus | 4 | 16 | 12.70 | 4.50 | 370 |
| | 5 | 32 | 10.70 | 3.50 | 238 |
| | 6 | 64 | 9.00 | 2.80 | 149 |
| Bronchi w/Cartilage in Wall | 7 | 128 | 7.60 | 2.30 | 91 |
| | 8 | 256 | 6.40 | 1.96 | 53 |
| | 9 | 512 | 5.40 | 1.54 | 34 |
| | 10 | 1024 | 4.60 | 1.30 | 20 |
| Terminal Bronchus | 11 | 2048 | 3.90 | 1.09 | 12 |
| | 12 | 4096 | 3.30 | 0.96 | 6.78 |
| Bronchiole w/muscle in wall | 13 | 8192 | 2.70 | 0.82 | 3.97 |
| | 14 | 16,384 | 2.30 | 0.74 | 2.20 |
| | 15 | 32,768 | 2.00 | 0.66 | 1.23 |
| Terminal Bronchiole | 16 | 65,536 | 1.65 | 0.60 | 0.68 |
| | 17 | 131,072 | 1.41 | 0.54 | 0.38 |
| Respiratory Bronchiole | 18 | 262,144 | 1.17 | 0.50 | 0.20 |
| | 19 | 524,288 | 0.99 | 0.47 | 0.11 |
| | 20 | 1,048,576 | 0.83 | 0.45 | 0.056 |
| Alveolar Duct | 21 | 2,097,152 | 0.70 | 0.43 | 0.030 |
| | 22 | 4,194,304 | 0.59 | 0.41 | 0.015 |
| Alveolar Sac | 23 | 8,388,608 | 0.50 | 0.41 | 0.008 |
| Alveoli. 21 Per duct | | 3E+0 | 0.23 | 0.28 | |

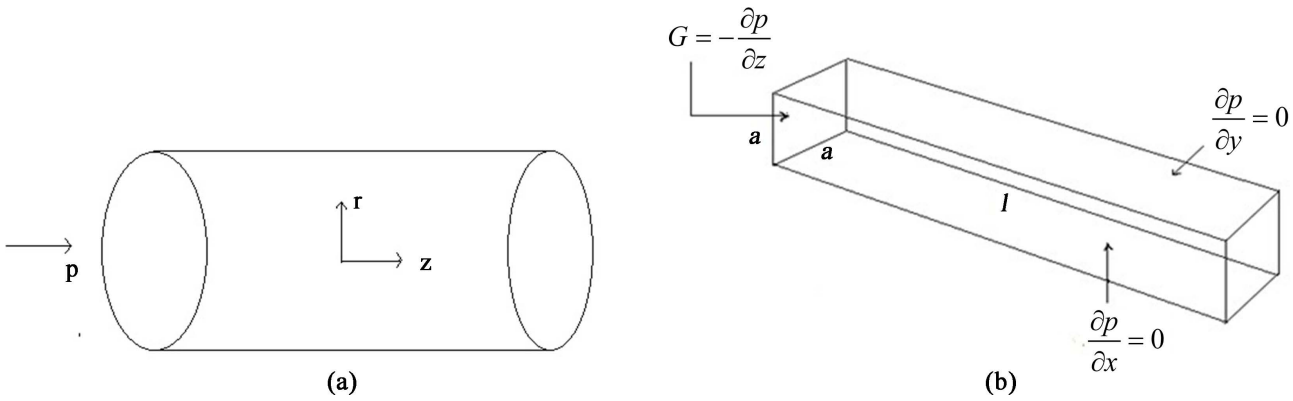


**Figure 2.** Geometry of the problem. (a) Cylindrical channel; (b) Square duct channel.

$$\rho\left[\frac{\partial v_r}{\partial t}+v\cdot\nabla v_r-\frac{1}{r}v_\theta^2\right]=-\frac{\partial p}{\partial r}+\mu\left[\nabla^2 v_r-\frac{v_r}{r^2}-\frac{2}{r^2}\frac{\partial v_\theta}{\partial\theta}\right]-\frac{\mu\varphi}{k}v_r \tag{3}$$

$\theta$-momentum

$$\rho\left[\frac{\partial v_\theta}{\partial t}+v\cdot\nabla v_\theta+\frac{1}{r}v_r v_\theta\right]=-\frac{\partial p}{\partial\theta}+\mu\left[\nabla^2 v_\theta-\frac{v_\theta}{r^2}+\frac{2}{r^2}\frac{\partial v_r}{\partial\theta}\right]-\frac{\mu\varphi}{k}v_\theta \tag{4}$$

$z$-momentum

$$\rho\left[\frac{\partial v_z}{\partial t}+v\cdot\nabla v_z\right]=-\frac{\partial p}{\partial z}+\mu\left[\nabla^2 v_z\right]-\frac{\mu\varphi}{k}v_z \tag{5}$$

where

$$v\cdot\nabla v_z=v_r\frac{\partial v_z}{\partial r}+\frac{1}{r}v_\theta\frac{\partial v_z}{\partial\theta}+\frac{\partial v_z}{\partial z} \tag{6}$$

$$\nabla^2 v_z=\frac{1}{r}\frac{\partial}{\partial r}\left(\frac{r\partial v_z}{\partial r}\right)+\frac{1}{r^2}\frac{\partial^2 v_z}{\partial\theta^2}+\frac{\partial^2 v_z}{\partial z^2} \tag{7}$$

We take the following assumptions: For steady flow

$$\frac{\partial v}{\partial t}=0 \tag{8}$$

The flow rate for radical and azimuthal components of the fluid are zero

$$\left(v_r=v_\theta=0\right). \tag{9}$$

For axisymmetric flow

$$\frac{\partial v}{\partial\theta}=0 \tag{10}$$

$$\frac{\partial p}{\partial\theta}=0 \tag{11}$$

The flow is fully developed. We have

$$\frac{\partial v_z}{\partial z}=0 \tag{12}$$

Then the continuity equation and angular momentum equation are identically satisfied.

From radial momentum equation we have.

$$\frac{\partial p}{\partial r}=0 \tag{13}$$

The pressure $p$ is a function of the axial co-ordinate $z$ only.

Then using Equation (6) and Equation (7) in Equation (5) we have

$$-\frac{\partial p}{\partial z}+\mu\frac{1}{r}\frac{\partial}{\partial r}\left(\frac{r\partial v_z}{\partial r}\right)-\frac{\mu\varphi}{k}v_z=0 \tag{14}$$

We use $v$ instead of $v_z$.

Then the axial momentum Equation (14) reduces to

$$-\frac{\partial p}{\partial z}+\mu\frac{1}{r}\frac{\partial}{\partial r}\left(\frac{r\partial v}{\partial r}\right)-\frac{\mu\varphi}{k}v=0 \tag{15}$$

$$\Rightarrow v = \frac{1}{1-\frac{\varphi}{4k}r^2}\left\{\frac{1}{4\mu}\frac{\partial p}{\partial z}r^2 + c_1 \ln r + c_2\right\} \tag{16}$$

where $c_1$ and $c_2$ are constants.

Here $v$ needs to be finite at $r = 0$, $c_1 = 0$.

The no slip boundary condition requires that $v = 0$ at $r = b$ (radius of the cylinder) which yields

$$c_2 = -\frac{1}{4\mu}\frac{\partial p}{\partial z}b^2 \tag{17}$$

From Equation (16) we get

$$\Rightarrow v = A\left\{\frac{G}{4\mu}\left(b^2 - r^2\right)\right\} \tag{18}$$

$$\text{Where } A = \frac{1}{1-\frac{\varphi}{4k}r^2} \text{ and } G = -\frac{\partial p}{\partial z} \tag{19}$$

Equation (18) gives the required solution for cylindrical channel of the porous medium.

### 3.2. Non-Porous Medium

For non-porous medium we take $\varphi = 0$ in Equation (3), Equation (4) and Equation (5). Then the axial momentum equation reduces to

$$-\frac{\partial p}{\partial z} + \mu\frac{1}{r}\frac{\partial}{\partial r}\left(\frac{r\partial v}{\partial r}\right) = 0 \tag{20}$$

$$\Rightarrow v = \frac{1}{4\mu}\frac{\partial p}{\partial z}r^2 + c_1 \ln r + c_2 \tag{21}$$

where $c_1$ and $c_2$ are constants.

Here $v$ must be finite at $r = 0$, $c_1 = 0$. The no slip boundary condition is $v = 0$ at $r = b$ (radius of the cylinder) which yields

$$c_2 = -\frac{1}{4\mu}\frac{\partial p}{\partial z}b^2 \tag{22}$$

From Equation (21) we get

$$v = \frac{G}{4\mu}\left(b^2 - r^2\right), \text{ Where } G = -\frac{\partial p}{\partial z} \tag{23}$$

Equation (23) gives the required solution for cylindrical channel of non-porous medium.

## 4. Results and Discussion

### 4.1. Porous Medium

Flow behavior in terminal bronchus of human lung for square duct channel and cylindrical channel with different parametric effects are discussed and compared in this section.

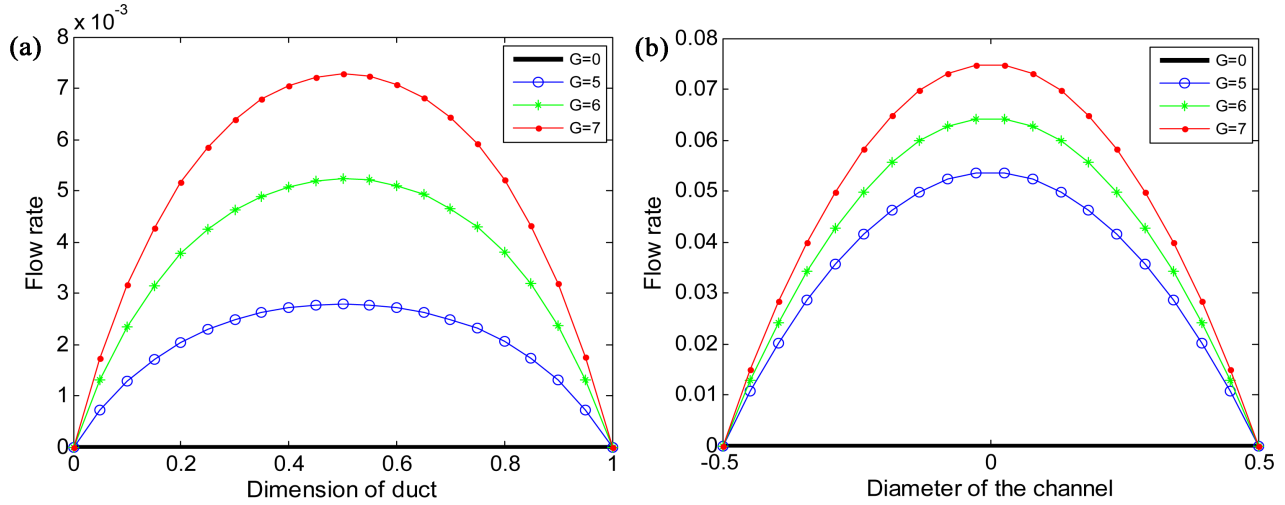


**Figure 3.** Variations of flow rate for different values of $G$ in (a) Square duct channel where $\mu = 0.4$, $\varphi = 0.7$, $k = 0.006$ and $c = 0.02$; (b) Cylindrical channel where $\mu = 0.4$, $\varphi = 0.7$, $k = 0.006$ and $b = 0.5$.

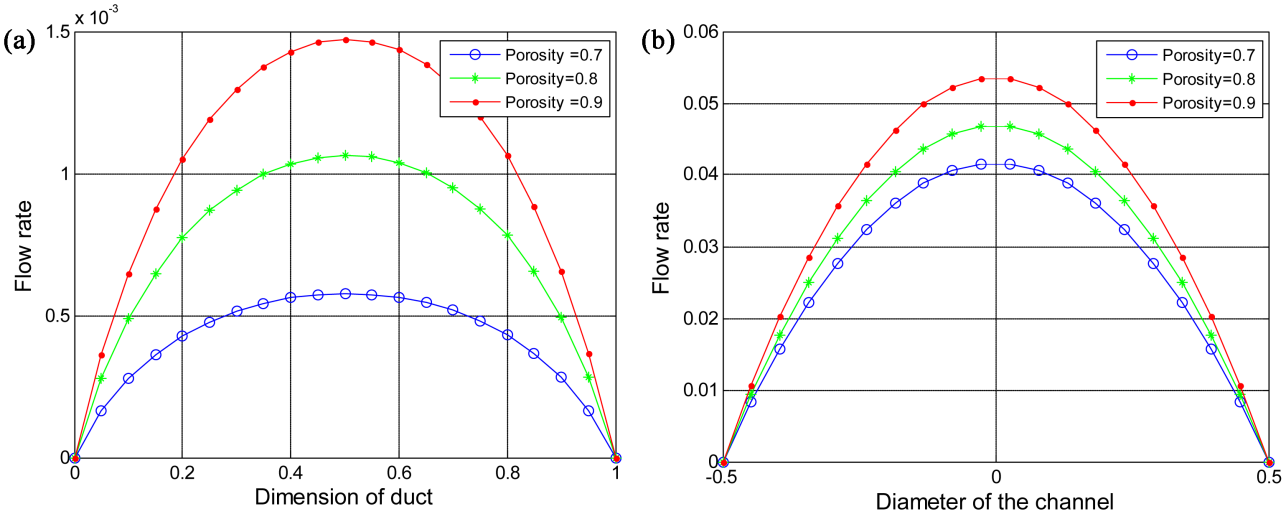


**Figure 4.** Variations of flow rate for different values of porosity ($\varphi$) in (a) Square duct channel where $G = 5$, $\mu = 0.4$, $k = 0.006$ and $c = 0.02$; (b) Cylindrical channel where $G = 5$, $\mu = 0.4$, $k = 0.006$ and $b = 0.5$.

**Figure 3** shows the flow rate in square duct channel and cylindrical channel for the same values of pressure gradient. For the increasing value of pressure gradient, the flow rate is increased in both channels. It can be noted that flow rate is increased much more in cylindrical channel than that of square duct channel for the same effect of pressure gradient and no flow take place when the pressure gradient is zero in both channels.

**Figure 4** shows the variations of flow rate for different values of porosity. If porosity is increased the flow rate is increased in both channels. Porosity represents the quality of pore to be porous.

If porosity is high then more amount of fluid will flow through the porous medium. It is also depicted in **Figure 4** that for the same value of porosity the flow rate is comparatively high in cylindrical channel than that of square duct

channel. The highest flow rates is found as 0.054 in cylindrical channel and it's about $1.48 \times 10^{-3}$ in square duct channel which is very small compared to cylindrical channel. The variations of flow rate with porosity effect in square duct channel and cylindrical channel are shown in Table 2.

Figure 5 shows the flow phenomena for different values of permeability parameter in both channels. Flow rate is decreased in square duct channel for lower value of permeability constant and increased in cylindrical channel for the higher value of permeability parameter. Permeability represents the flow ability of the fluid to flow through per unit area of porous medium. It is also noted that in cylindrical channel the highest flow rate is measured as 0.0704 and in square duct channel it's about $1.478 \times 10^{-3}$. So the flow rate is higher in cylindrical channel compared to square duct channel for the same value of permeability parameter. The variations of flow rate with permeability parameter are shown in Table 3.

Figure 6 shows the flow behavior in both channels for the effect of viscosity. It is observed that for the same value of viscosity the flow rate is more in cylindrical channel compared to square duct channel. In square duct channel as shown in Figure 6(a) the flow rate is decreased by 0.3 compared to cylindrical channel shown in Figure 6(b). For increasing the value of viscosity from 0.4 to 0.5 the flow rate is decreased in Figure 6(c) by 0.25 compared to Figure 6(d). Flow rate

Table 2. Flow rate with porosity effect ( $\varphi$ ) in square duct channel and cylindrical channel.

| Porosity value ($\phi$) | Square duct channel m/s | Cylindrical channel m/s |
|---|---|---|
| 0.7 | $0.521 \times 10^{-3}$ | 0.041 |
| 0.8 | $1.21 \times 10^{-3}$ | 0.047 |
| 0.9 | $1.48 \times 10^{-3}$ | 0.054 |

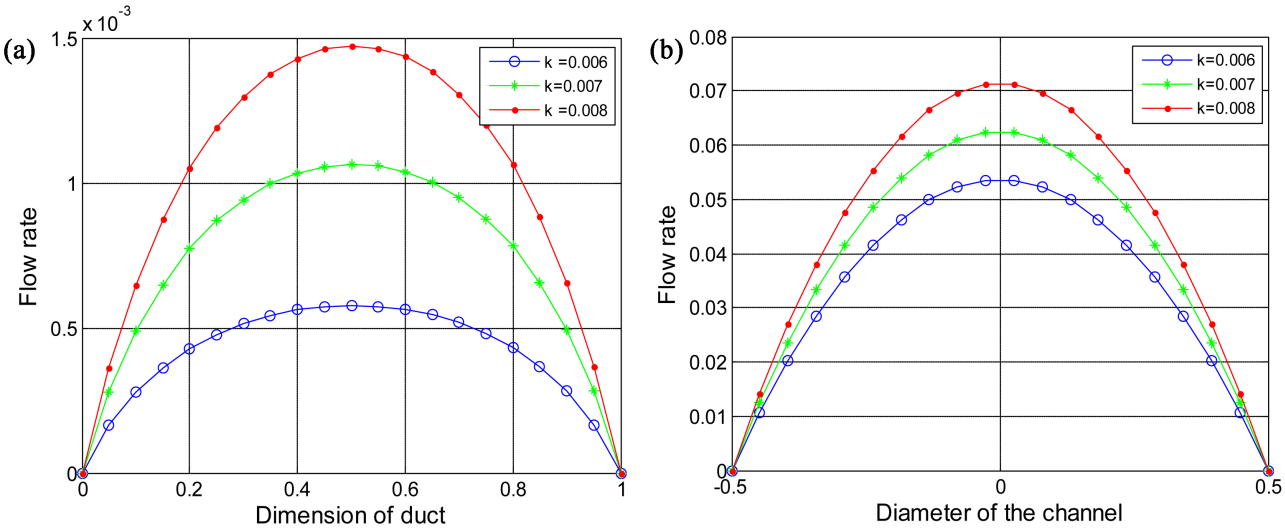


Figure 5. Variations of flow rate for different values of $k$ in (a) Square duct channel where $G=5$, $\mu=0.4$, $\varphi=0.7$ and $c=0.02$ (b)Cylindrical channel where $G=5$, $\mu=0.4$, $\varphi=0.7$ and $b=0.5$.

**Table 3.** Flow rate with permeability effect ($k$) in square duct channel and cylindrical channel.

| Permeability ($k$) $m^2$ | Square duct channel m/s | Cylindrical channel m/s |
|---|---|---|
| 0.006 | $0.528 \times 10^{-3}$ | 0.0528 |
| 0.007 | $1.232 \times 10^{-3}$ | 0.0616 |
| 0.008 | $1.478 \times 10^{-3}$ | 0.0704 |

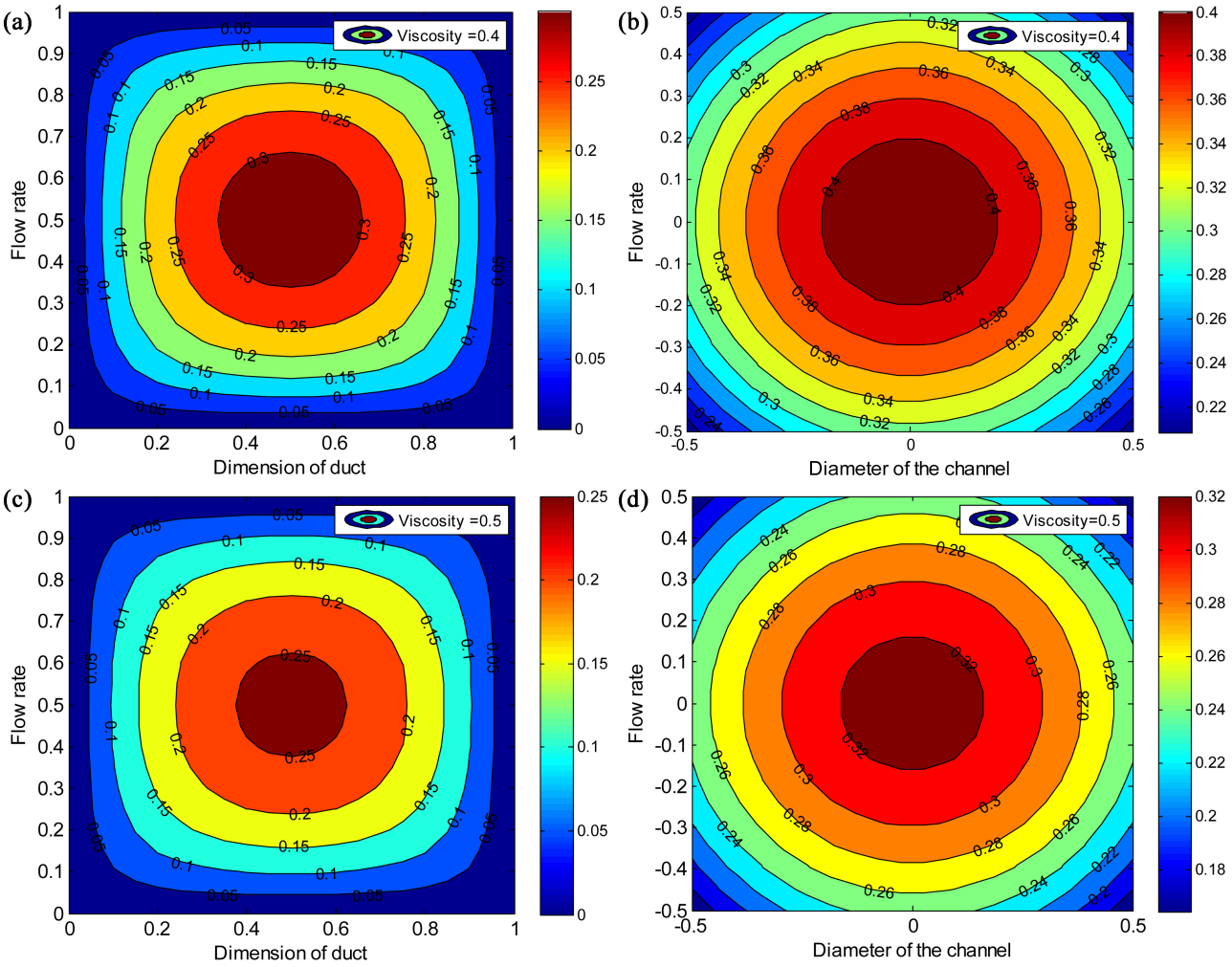


**Figure 6.** ((a), (b)) Variations of flow rate in both channels for same value of viscosity where $\mu = 0.4$, $G = 5$, $\varphi = 0.7$ and $k = 0.006$. (a) Square duct channel; (b) Cylindrical channel; ((c), (d)) Variations of flow rate in both channels for the same value of viscosity where $\mu = 0.5$, $G = 5$, $\varphi = 0.7$ and $k = 0.006$. (c) Square duct channel; (d) Cylindrical channel.

is decreased in both channels for increasing the value of viscosity. It is also noticed that for the same channel as square duct the flow rate is decreased in **Figure 6(c)** compared to **Figure 6(a)** and also for cylindrical channel the flow rate is decreased in **Figure 6(d)** compared to **Figure 6(b)** for increasing the value of viscosity. So, it can be noted that the flow rate is a decreasing function of viscosity and it is decreased more in square duct channel compared to cylindrical

channel.

### 4.2. Non-Porous Medium

The governing equations have been solved numerically for both channels in non-porous medium. Figure 7 shows the flow phenomena for different values of pressure gradient in square duct channel and cylindrical channel for non-porous medium. Here the flow rate is increased in both channels for increasing value of pressure gradient and the flow rate is considerably very high in cylindrical channel compared to square duct channel for the same value of pressure gradient. The maximum flow rate is measured as $3.704 \times 10^{-3}$ in square duct channel and in cylindrical channel it's about 2.116 in non-porous medium.

The variations of flow rate in both channels for non-porous medium are shown in Table 4.

## 5. Error Analysis

The percentage error of the problem of cylindrical Channel is estimated (Table 5). The differential equation is solved analytically and numerically. The error of the problem is analyzed with analytical and numerical solutions.

Figure 8(b) shows the error in the flow rate. It is observed that the error at the center and the boundary of the channel is found as zero because the boundary

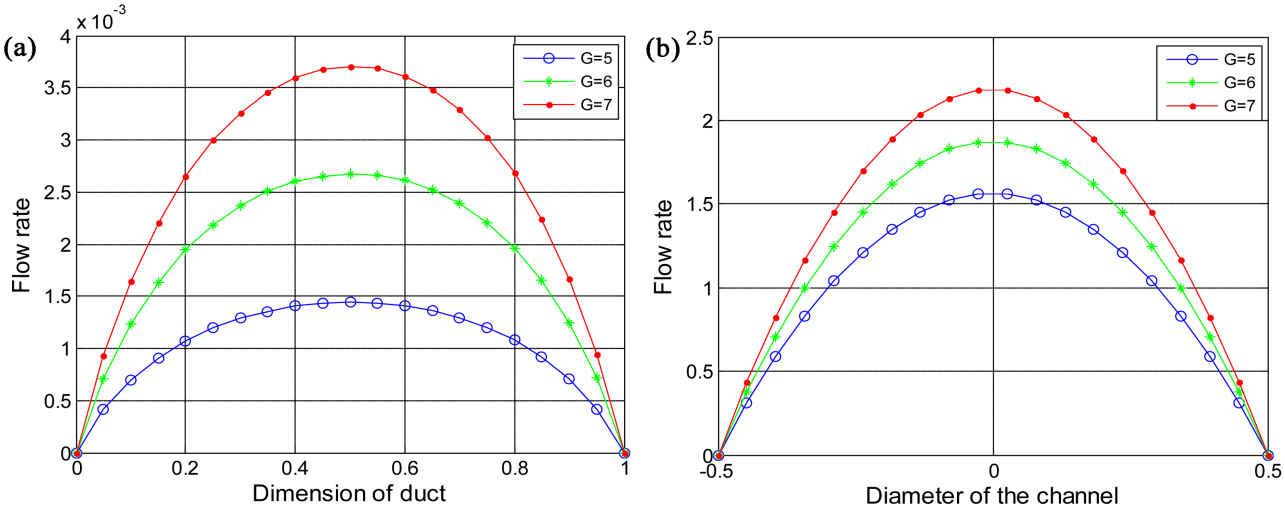


Figure 7. Variations of flow rate for different values of $G$ in (a) Square duct channel where $c = 0.02$ and (b) Cylindrical channel where $\mu = 0.4$ and $b = 0.5$.

Table 4. Flow rate with pressure gradient ($G$) in both channels for non-porous medium.

| Pressure gradient ($G$) Pa | Square duct channel m/s | Cylindrical channel m/s |
|---|---|---|
| 5 | $1.341 \times 10^{-3}$ | 1.565 |
| 6 | $2.694 \times 10^{-3}$ | 1.837 |
| 7 | $3.704 \times 10^{-3}$ | 2.116 |

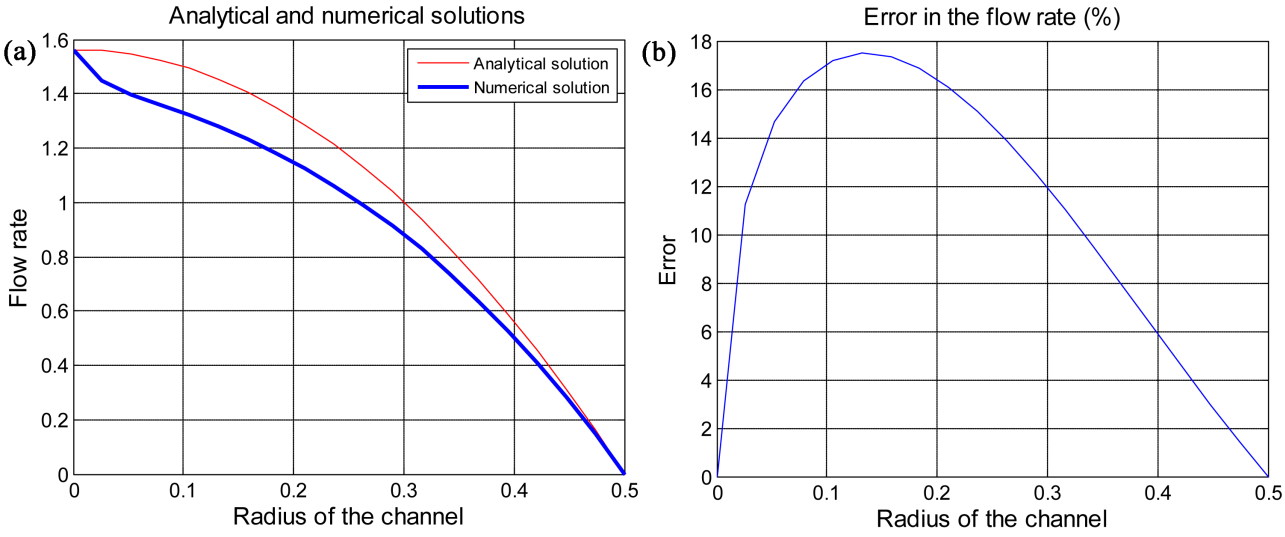


**Figure 8.** Error in flow rate for cylindrical channel.

**Table 5.** Error estimation along radial distance of cylindrical channel flow.

| Radius | Analytical solution | Numerical solution | Error (%) |
|---|---|---|---|
| 0 | 1.5625 | 1.5625 | 0 |
| 0.025 | 1.5615 | 1.3710 | 12.2 |
| 0.050 | 1.5605 | 1.3327 | 14.6 |
| 0.075 | 1.5595 | 1.3044 | 16.36 |
| 0.100 | 1.5525 | 1.2853 | 17.21 |
| 0.125 | 1.4782 | 1.2197 | 17.48 |
| 0.150 | 1.4362 | 1.1872 | 17.34 |
| 0.175 | 1.3925 | 1.1569 | 16.92 |
| 0.20 | 1.3483 | 1.1299 | 16.20 |
| 0.25 | 1.1852 | 1.0180 | 14.10 |
| 0.30 | 1.000 | 0.8799 | 12.01 |
| 0.35 | 0.7835 | 0.7146 | 8.80 |
| 0.40 | 0.5678 | 0.5348 | 5.81 |
| 0.45 | 0.3128 | 0.3040 | 2.81 |
| 0.50 | 0 | 0 | 0 |

condition is applied. From center to boundary the error is at first increased and then gradually decreased. It is observed that the error is 0% at the point zero and increased very gradually. After a certain point error is decreased and enriched to zero. The maximum error is 17.48% at 0.125 and the minimum error is 0% at 0.5 along the radius of the channel.

## 6. Conclusions

Flow behavior is observed in human lung for cylindrical channel of porous and

non-porous medium. The analytical solution is obtained by taking cylindrical coordinates of the system. The numerical results of the cylindrical channel are compared with square duct channel for the same condition of different parametric effect. For both channels flow rate is also measured in non-porous medium. We conclude the following:

The flow rate increases in cylindrical channel compared to square duct channel for the same effect of pressure gradient, porosity and permeability parameters. The results help to set a point that gas exchange in cylindrical channel is accelerated in cylindrical channel than that in duct channel.

## Acknowledgements

The authors are grateful to the anonymous referees for their valuable comments and constructive suggestions of the manuscript.

## Conflicts of Interest

The authors declare no conflicts of interest regarding the publication of this paper.

## References

[1] Calay, R.K., Kurujareon, J. and Holdo, A.E. (200) Numerical Simulation of Respiratory Flow Patterns within Human Lung. *Respiratory Physiology & Neurobiology*, **130**, 201-221. https://doi.org/10.1016/S0034-5687(01)00337-1

[2] Freitas, R.K. and Schroder, W. (2008) Numerical Investigation of the Three-Dimensional Flow in a Human Lung Model. *Journal of Biomechanics*, **41**, 2446-2457. https://doi.org/10.1016/j.jbiomech.2008.05.016

[3] Liu, Y., So, R.M.C. and Zhang, C.H. (2003) Modeling the Bifurcating Flow in an Asymmetric Human Lung Airway. *Journal of Biomechanics*, **36**, 951-959. https://doi.org/10.1016/S0021-9290(03)00064-2

[4] Hirahara, H., Iwazaki, K., Ahmmed, M.U. and Nakamura, M. (2011) Numerical Analysis of Air Flow in Dichotomous Respiratory Channel with Asymmetric Compliance under HFOV Condition. *Journal of Fluid Science and Technology*, **6**, 932-948. https://doi.org/10.1299/jfst.6.932

[5] Akhter, S. and Ahmmed, M. (2022) Study on Flow Behavior in Terminal Bronchus of Human Lung for Porous Medium. *Journal of Bangladesh Mathematical Society*, **42**, 69-80. https://doi.org/10.3329/ganit.v42i1.61001

[6] Kuwahara, F., Sano, Y., Liu, J.J. and Nakayama, A. (2009) A Porous Media Approach for Bifurcating Flow and Mass Transfer in a Human Lung. *Journal of Heat Transfer*, **131**, 1013-1024. https://doi.org/10.1115/1.3180699

[7] DeGroot, C.T. and Straatman, A.G. (2012) Towards a Porous Media Model of the Human Lung. 4*th International Conference on Porous Media and Its Applications*, **1453**, 69-74. https://doi.org/10.1063/1.4711155

[8] DeGroot, C.T. and Straatman, A.G. (2018) A Porous Media Model of Alveolar Duct Flow in the Human Lung. *Journal of Porous Media*, **21**, 405-422. https://doi.org/10.1615/JPorMedia.v21.i5.20

[9] Tang, H.T. and Fung, Y.C. (1975) Fluid Movement in a Channel with Permeable Walls Covered by Porous Media. *Journal of Applied Mechanics*, **42**, 45-50.

https://doi.org/10.1115/1.3423551

[10] Leontiev, A.I., Zditovets, A.G., Kiselev, N.A., Vinogradov, Yu.A. and Strongin, M.M. (2019) Experimental Investigation of Energy (Temperature) Separation of a High Velocity Air Flow in a Cylindrical Channel with a Permeable Wall. *Experimental Thermal and Fluid Science*, **105**, 206-215. https://doi.org/10.1016/j.expthermflusci.2019.04.002

[11] Heidarinejad, G., Roozbahani, M.H. and Heidarinejad, M. (2019) Studying Airflow Structures in Periodic Cylindrical Hills of Human Tracheal Cartilaginous Rings. *Respiratory Physiology & Neurobiology*, **266**, 103-114. https://doi.org/10.1016/j.resp.2019.04.012

[12] Yu, C.P. and Chandra, K. (1978) Deposition of Charged Particles from Laminar Flows in Rectangular and Cylindrical Channels by Image Force. *Journal of Aerosol Science*, **9**, 175-180. https://doi.org/10.1016/0021-8502(78)90077-0

[13] Fukagata, K. and Kasagi, N. (2002) Highly Energy Conservative Finite Difference Method for the Cylindrical Coordinate System. *Journal of Computational Physics*, **181**, 478-498. https://doi.org/10.1006/jcph.2002.7138

[14] Verzicco, R. and Orlandi, P. (1996) A Finite Difference Scheme for Three Dimensional Incompressible Flows in Cylindrical Coordinates. *Journal of Computational Physics*, **123**, 402-414. https://doi.org/10.1006/jcph.1996.0033

## Nomenclature

| Symbol | Meaning |
|---|---|
| $v$ | Flow rate, m/s |
| $p$ | Pressure, Pa |
| $r$ | Radial component |
| $\theta$ | Azimuthal component |
| $z$ | $z$-axis |
| $v_r$ | Radial component of fluid velocity, m/s |
| $v_\theta$ | azimuthal component of fluid velocity, m/s |
| $v_z$ | Axial fluid velocity, m/s |
| $R$ | Darcy resistance (a measure of the resistance to airflow) $kg \cdot m^{-2} \cdot s^{-2}$ |
| $\Delta$ | Change in a quantity |
| $\mu$ | Base fluid viscosity, kg/ms |
| $\varphi$ | Porosity (represents the ratio of pore volume to the total volume) |
| $k$ | Permeability (indicates the ability of fluids to flow through porous medium), $m^2$ |
| $b$ | Radius of cylindrical channel, m |